Electronic Supplementary Information

MoS_2 nanosheets vs nanowires: preparation and theoretical study of highly stable and efficient nanofluids for Concentrating Solar Power

Javier Navas,*[,1] Paloma Martínez-Merino,[1] Antonio Sánchez-Coronilla,*[,2] Juan Jesús Gallardo,[1] Rodrigo Alcántara,[1] Elisa I. Martín,[3] José C. Piñero,[4] Juan R. León,[2] Teresa Aguilar,[1] José Hidalgo Toledo,[2] Concha Fernández-Lorenzo[1]

[1] Departamento de Química Física, Facultad de Ciencias, Universidad de Cádiz, E-11510 Puerto Real (Cádiz), Spain;
[2] Departamento de Química Física, Facultad de Farmacia, Universidad de Sevilla, E-41012 Sevilla, Spain;
[3] Departamento de Ingeniería Química, Facultad de Química, Universidad de Sevilla, E-41012 Sevilla, Spain.
[4] Departamento de Ciencias de los Materiales, Ingeniería Metalúrgica y Química Inorgánica, Universidad de Cádiz, E-11510 Puerto Real (Cádiz), Spain

S1. Calculations of the ratio of the polar and dispersive components of the surface tension for the surfactants used

The liquid phase exfoliation (LPE) process is favoured when the solid-liquid surface tension is minimized. According to the OWRK [1] theory for surface tension, and the studies of Fowkes [2], γ_{SL} can be defined as

$$\gamma_{SL} = \gamma_S^p + \gamma_S^d + \gamma_L^p + \gamma_L^d - 2\sqrt{\gamma_S^p \gamma_L^p} - 2\sqrt{\gamma_S^d \gamma_L^d} \qquad \text{(S1)}$$

where γ_S^p, γ_L^p, γ_S^d and γ_L^d are the polar and dispersive components of the surface tension of the solid and liquid. According to equation (S1), for minimizing γ_{SL}, the values of γ_S^p and γ_L^p and also the values of γ_S^d and γ_L^d must be as close as possible. Alternatively, the equation (S1) can be expressed as

$$\gamma_{SL} = \left(\frac{\gamma_S^p}{\gamma_S^d} + 1\right)\gamma_S^d + \left(\frac{\gamma_L^p}{\gamma_L^d} + 1\right)\gamma_L^d - 2\left(\sqrt{\frac{\gamma_S^p \gamma_L^p}{\gamma_S^d \gamma_L^d}} + 1\right)\sqrt{\gamma_S^d \gamma_L^d} \qquad \text{(S2)}$$

Taking into account this equation, to minimize γ_{SL} the values of the ratios γ_S^p/γ_S^d and γ_L^p/γ_L^d should be closer, as should the values of the components γ_S^d and γ_L^d.

Thus, in our case, the ratio of the polar and dispersive components of the MoS_2 2D nanostructure is 0.449, as reported previously [3]. Thus, it is necessary to calculate the polar and dispersive components for the base fluid, which is the mixture of the HTF and the surfactant, and also the value of the surface tension. The components can be obtained from the studies of Young [4] and Good et al. [5], which led to

$$\sqrt{\gamma_R^d \gamma_L^d} + \sqrt{\gamma_R^p \gamma_L^p} = \frac{\gamma_L(1 + cos\theta)}{2} \qquad \text{(S3)}$$

where θ is the contact angle and, in this case, R is referred to a solid used as a reference. A Teflon support is used as reference, and their tension surface components were characterized following the procedure described in [3]. The values obtained were γ_R^p=0.07

mN·m^{-1}, and γ_R^p=24.6 mN·m^{-1}. The value of γ_R^p is close to zero, and this makes it possible to obtain the components from equation (S3) and from the experimental values of the surface tension and the contact angle. The surface tension was measured by means of stalagmometry and the contact angle using a handmade system assembled in our lab.

First, following the procedure described, the surface tension and their components were estimated for the HTF used, which is the eutectic mixture of diphenyl oxide and biphenyl. Table S1 shows the values obtained including the value for the ratio of the polar and dispersive components.

Table S1. Values of the surface tension and their components and the ratio between them for the HTF used.

Liquid	$\boldsymbol{\gamma_L}$ **/ mN m^{-1}**	$\boldsymbol{\gamma_L^p}$ **/ mN m^{-1}**	$\boldsymbol{\gamma_L^d}$ **/ mN m^{-1}**	$\boldsymbol{\gamma_L^p/\gamma_L^d}$
HTF	39.96	16.46	23.50	0.70

Furthermore, several surfactants were tested to adjust the ratio of the components of the liquid to that of the solid, i.e. the MoS_2 2D nanostructures. These surfactants were benzalkonium chloride (BAC, Sigma-Aldrich©), 1-octadecanethiol (ODT, purity: 98%, density 847 kg m^{-3} at 298 K, Sigma-Aldrich©), polyvinylpyrrolidone (PVP, average molecular weight: 4000, Sigma-Aldrich©), and polyethylene glycol (PEG, average molecular weight: 4000, Sigma-Aldrich©). Several concentrations were tested for each surfactant. Table S2 shows the most relevant values obtained for the surface tension, their components and the ratio. From these results, the surfactants BAC and PVP were discarded because they did not suitably modify the surface tension and its components. The addition of ODT and PEG modified the surface tension and its components, and the values obtained for the ratio of the components are close to the ratio for MoS_2 2D nanostructures (0.449), as is observed in Table S2.

Therefore, three nanofluids were prepared by means of the LPE process: the first using ODT with a concentration of $7.2 \cdot 10^{-3}$ wt.%; the second using PEG as surfactant with a concentration of $1.2 \cdot 10^{-1}$ wt.%; and one without surfactant for comparison purposes.

Table S2. Values of the surface tension and their components and the ratio between them for the HTF used.

Surfactant	**Concentration / wt.%**	γ_L **/ mN m^{-1}**	γ_L^p **/ mN m^{-1}**	γ_L^d **/ mN m^{-1}**	γ_L^p/γ_L^d
BAC	$1.3 \cdot 10^{-3}$	40.45	17.39	23.05	0.755
ODT	$7.2 \cdot 10^{-3}$	39.04	11.57	27.48	0.421
PVP	$1.0 \cdot 10^{-2}$	41.81	17.08	24.73	0.691
PEG	$1.2 \cdot 10^{-1}$	38.55	12.75	25.79	0.494

S2. Details of the stability characterization

Stability is one of the key concepts in nanofluids because their thermal properties depend heavily on whether they are stable or unstable. UV-vis spectroscopy can provide a measurable characterization of stability by evaluating the extinction coefficient of a suspension [6]. To this end, UV-vis spectra were recorded using a DH-2000-Bal halogen lamp supplied by Ocean Optics© and a USB-2000+ monochromator supplied by Ocean Optics operating in the range of wavelength of 400-880 nm, using a glass cuvette at room temperature.

Particle size and size distribution was also measured by Zetasizer Nano ZS, using the principle of dynamic light scattering (DLS) as a simple method for analysing suspension stability and particle size measurements in solution [7, 8]. This technique usually overestimates the values of the particle size because the value obtained corresponds to the hydrodynamic diameter, which is estimated as the sum of the particle size and the Debye length. The Debye length is the thickness of the diffuse layer, a layer of species between the surface of the nanoparticle and the slipping plane that moves with the nanoparticle within the base fluid [9].

Finally, stability measurements were performed for eight days. Several measurements were performed each day, each one in triplicate.

S3. Theoretical analysis. Stability of the surfactants with the MoS_2 nanosheet

The analysis of the interaction between surfactant molecules and the surface of a nanosheet of MoS_2 is discussed below.

The interaction between the extremes of the surfactant molecules and the monolayer (001) surface of MoS_2 was studied. The interaction in parallel with their H atoms over the surface was also analysed (see Figures S1 and S2). For the interaction through the extremes, in the case of ODT the extremes studied were -SH and methyl groups, while the -OH group was studied for the interaction with PEG. The interaction sites with the nanosheet surface are shown in Figures S1 and S2. For the interaction with the surface, three binding sites were studied which were defined by taking as the reference point the H of the H-X group (X=O, S, CH_2) over a Mo atom (**1**, **4** for ODT in Figure S1 and **8** for PEG in Figure S2), over the gap between three S and Mo (**2**, **5** for ODT in Figure S1 and **9** for PEG in Figure S2), and over a S atom (**3**, **6** for ODT in Figure S1 and **10** for PEG in Figure S2). For the parallel interaction with the monolayer, the structures are **7** and **11** for ODT and PEG, respectively, in Figures S1 and S2. In the interests of clarity, the images in Figures S1 and S2 only include the terminal region of the surfactant molecule that interacts with the surface in structures **1-6** for ODT, and **8-10** for PEG.

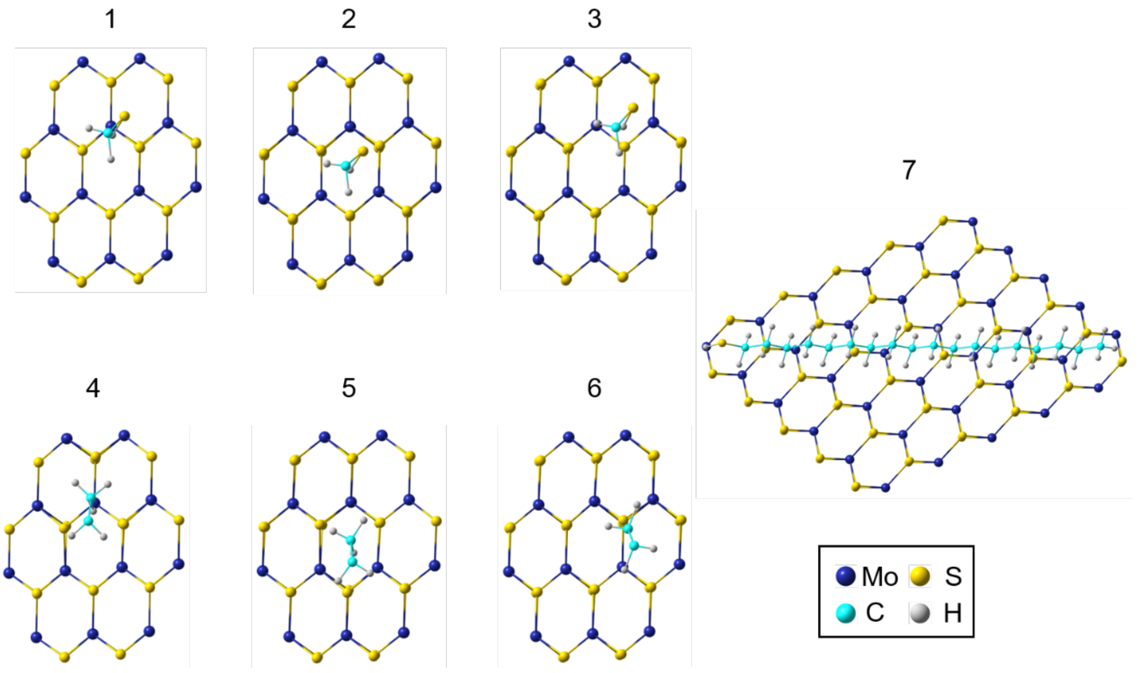

Figure S1. The local geometry in 2D for the interaction of ODT with the MoS2 (001) surface.

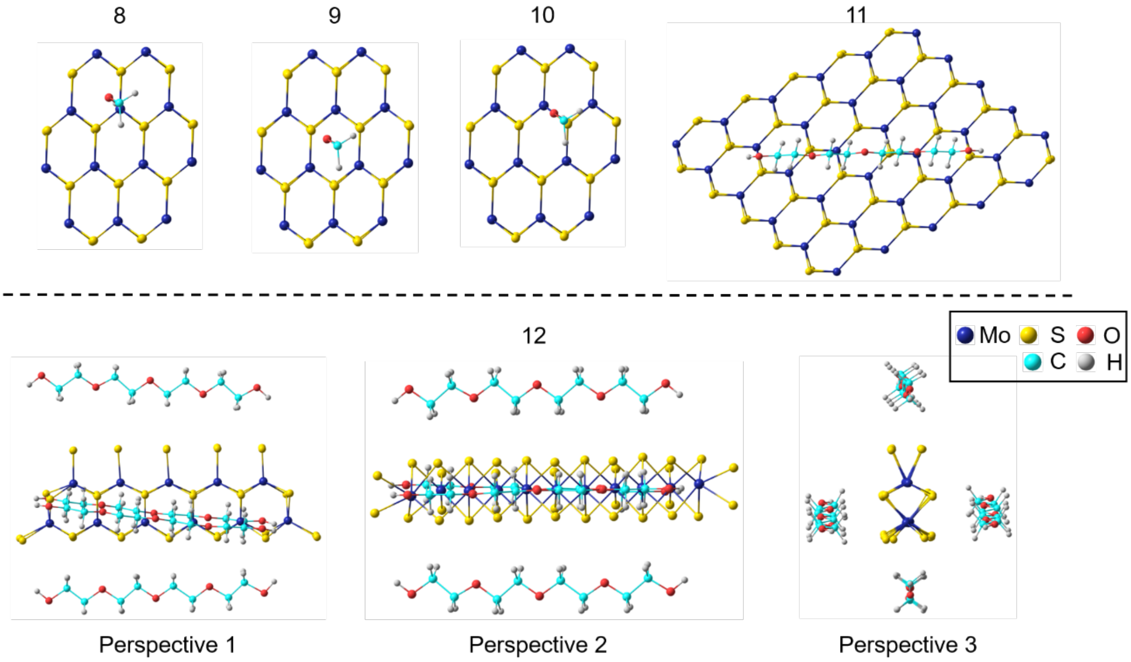

Figure S2. The local geometry in 2D for the interaction of PEG with the MoS2 (001) surface (from **8** to **11**) and the interaction of the wire with four PEG molecules (**12**).

Table S3 includes the interaction energies (E_{int}) associated with each binding site. This E_{int} is defined as

$$E_{int} = E_{(MoS_2 + surfactant)} - E_{(MoS_2)} - E_{(surfactant)} \qquad \text{(S4)}$$

where $E_{(MoS_2 + surfactant)}$, $E_{(MoS_2)}$ and $E_{(surfactant)}$ are the total energies of the surfactant with the monolayer (001) surface of MoS_2, the bare (001) surface of MoS_2 and the surfactant, respectively. In terms of energy, the most stable interaction of both surfactants with the surface of the MoS_2 involves the binding site on top of the Mo. In addition, the interactions of the MoS_2 with PEG are favoured to those with ODT (see Table S3). For the interaction of the surfactants in parallel to the surface, the interaction is more favourable with the PEG (**11**) than with the ODT (**7**) molecule.

Table S3. Interaction energy associated with each binding site shown in Figures S1 and S2.

Position	Figure S4	E_{int} (kcal/mol)	Figure S5	E_{int} (kcal/mol)
Over Mo	**1**	6.712	**8**	-2.523
Over the gap	**2**	13.910	**9**	-0.065
Over S	**3**	9.685	**10**	-0.058
Over Mo (H-CH_2)	**4**	72.128		
Over the gap (H-CH_2)	**5**	46.682		
Over S (H-CH_2)	**6**	50.065		
Parallel	**7**	48.422	**11**	15.849
Wire			**12**	-242.412

S4. UV-vis spectra obtained in the stability analysis

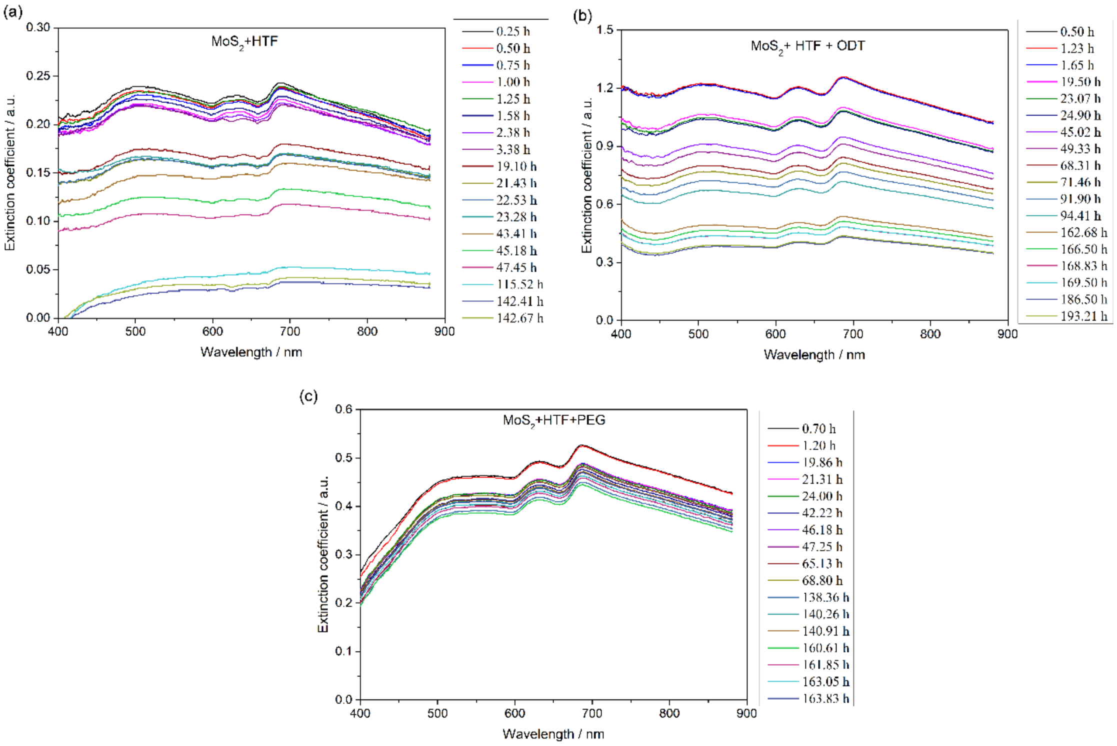

Figure S3. Plots of some of the UV-vis recorded for the nanofluid obtained without surfactant (a), and using ODT (b) and PEG (c) as surfactants.

S5. *Figure of Merit* for laminar flow conditions

For laminar flow conditions, the typical *Figure of Merit* gives the ratio between the increase in viscosity and the increase in thermal conductivity. When the increase in dynamic viscosity (*IDV*) is less than four times the thermal conductivity enhancement (*TCE*), an improvement in the working conditions is obtained [10]. Mathematically, this can be expressed as

$$\frac{IDV}{TCE} = \frac{\left(\mu_{nf} - \mu_{bf}\right)/\mu_{nf}}{\left(k_{nf} - k_{bf}\right)/k_{nf}} \tag{S5}$$

where μ is the dynamic viscosity, k is the thermal conductivity, and the subscripts *nf* and *bf* refer to the nanofluid and the base fluid, respectively. Thus, Figure S4 shows the values obtained for the *IDV*/*TCE* ratio for the nanofluids based on MoS_2 nanosheets (prepared using ODT) and on MoS_2 nanowires (prepared using PEG). Both nanofluids show values below 4 in all the temperature ranges, which means the nanofluids improved the efficiency of the base fluid.

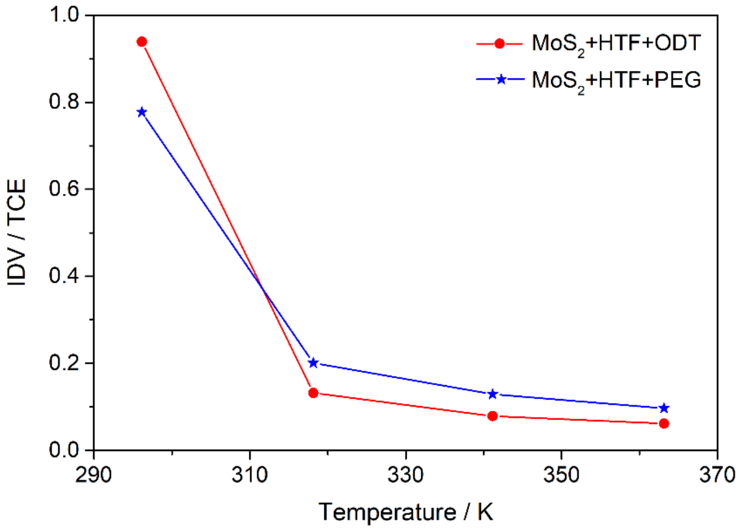

Figure S4. Ratio between the increase in dynamic viscosity and the thermal conductivity enhancement which is used as a *FoM* for laminar flow conditions.

S6. *Figure of Merit* for turbulent flow conditions. Dittus-Boelter equation

Under turbulent flow conditions, two *FoMs* can be considered: the ratio of the heat transfer coefficient between nanofluids and the base fluid according to the Dittus-Boelter equation, and the ratio of the Mouromtseff number. Both *FoMs* supply similar results. The *FoM* based on the ratio of the Mouromtseff number is analysed in the manuscript. Below, the *FoM* based on Dittus-Boelter equation is analysed.

The Dittus-Boelter equation gives the ratio of the heat transfer coefficient of the nanofluids and the base fluid [11]. Mathematically, it can be expressed as

$$FoM = \frac{h_{nf}}{h_{bf}} = \left(\frac{\rho_{nf}}{\rho_{bf}}\right)^{0.8} \left(\frac{k_{nf}}{k_{bf}}\right)^{0.6} \left(\frac{C_{P,nf}}{C_{P,bf}}\right)^{0.4} \left(\frac{\mu_{nf}}{\mu_{bf}}\right)^{-0.4} \tag{S6}$$

where μ, k and the subscripts have been defined before, h is the heat transfer coefficient, ρ is the density, and C_P is the isobaric specific heat. If $h_{nf} / h_{bf} > 1$, the efficiency of the heat transfer process is improved. This occurs when an increase in density, isobaric specific heat and thermal conductivity is obtained for the nanofluids. However, an increase in dynamic viscosity leads to a decrease in the efficiency of the heat transfer process. Thus, Figure S5 shows the values obtained for the ratio of the heat transfer coefficient for the nanofluids based on MoS_2 nanosheets (prepared using ODT) and on MoS_2 nanowires (prepared using PEG). It is possible to observe an increase in the efficiency of up to 35% for the nanofluid based on MoS_2 nanosheets and of up to 25% for the nanofluid based on MoS_2 nanowires.

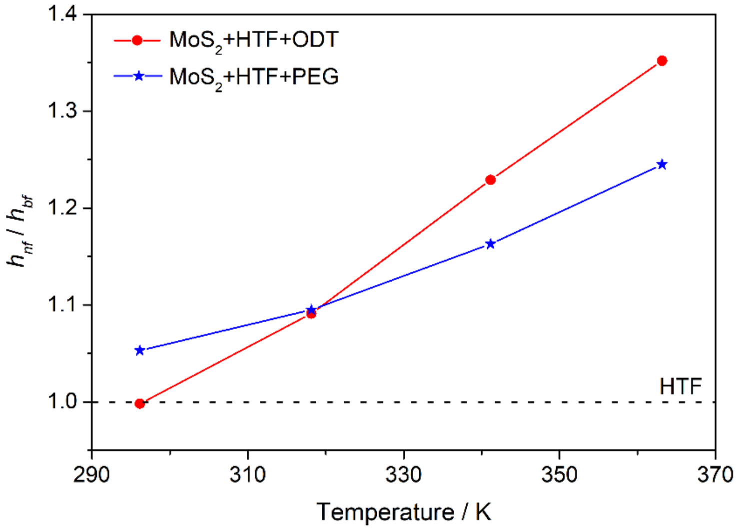

Figure S5. Ratio between the heat transfer coefficient of the nanofluids and the base fluid.

References

1. D. K. Owens, *J Appl Polym Sci*, 1970, **14**, 1725-&.
2. F. M. Fowkes, *Ind Eng Chem*, 1964, **56**, 40-&.
3. J. F. Shen, Y. M. He, J. J. Wu, C. T. Gao, K. Keyshar, X. Zhang, Y. C. Yang, M. X. Ye, R. Vajtai, J. Lou and P. M. Ajayan, *Nano Lett*, 2015, **15**, 5449-5454.
4. T. Young, *Philosophical Transactions*, 1805, **95**, 65-87.
5. R. J. Good and L. A. Girifalco, *J Phys Chem-Us*, 1960, **64**, 1960-1960.
6. W. S. Sarsam, A. Amiri, M. N. M. Zubir, H. Yarmand, S. N. Kazi and A. Badarudin, *Colloid Surface A*, 2016, **500**, 17-31.
7. S. A. Angayarkanni and J. Philip, *Adv Colloid Interfac*, 2015, **225**, 146-176.
8. R. C. Murdock, L. Braydich-Stolle, A. M. Schrand, J. J. Schlager and S. M. Hussain, *Toxicol Sci*, 2008, **101**, 239-253.
9. Y. Y. Song, H. K. D. H. Bhadeshia and D. W. Suh, *Powder Technol*, 2015, **272**, 34-44.
10. R. Prasher, D. Song, J. L. Wang and P. Phelan, *Appl Phys Lett*, 2006, **89**.
11. F. W. Dittus and L. M. K. Boelter, *University California Publications Eng.*, 1930, **2**, 443-461.